

## Barrier Theory of the Photoconductivity of Lead Sulfide\*

J. C. SLATER

*Massachusetts Institute of Technology, Cambridge, Massachusetts*

(Received April 16, 1956)

The barrier theory of the infrared photoconductivity of PbS films is discussed, according to which the high resistance of the films arises from  $n$ - $p$ - $n$  barriers at the surfaces between the crystallites forming the films, the barriers being formed in the oxidizing process used in preparing the films. Under the action of light, electron hole pairs are formed, these carriers become trapped in the  $n$ - and  $p$ -type regions, respectively, the resulting charge density lowers the barriers, and hence the conductivity is increased. This theory is worked out quantitatively, and compared with experimental results of Mahlman on films of the type actually used as sensitive photoconductors. The theory shows good qualitative and quantitative agreement with experiment in numerous respects, including the explanation of the dark conductivity of the films and its dependence on temperature, the photoconductivity as a function of irradiance and temperature, the time constants involved in the rise or decay of the photoconductivity, and the short-wave limit of the photoconductivity. In working out the theory of the barrier model, we use the properties of the bulk material as determined by Petritz and Scanlon, and the properties of the films are found to be consistent with our knowledge of the behavior of the bulk material.

### 1. INTRODUCTION

LEAD sulfide films are among the most sensitive infrared photoconductors known. One of the suggested explanations<sup>1</sup> is that in the dark there are barriers interposed between different crystallites of the film, which increase the resistivity beyond that of the bulk material, and that illumination reduces the height of these barriers, increasing the conductivity. It is the purpose of the present paper to work out some details of this barrier theory, and to show that in fact it is capable of describing many of the observed features of PbS photoconductivity. It is not claimed in any way that the barrier effect is the only mechanism present in PbS. Other mechanisms for photoconductivity are well known; Rose<sup>2</sup> has given a good description of them, and has concluded that it is hardly possible to deduce the mechanism uniquely from an experimental study of photoconductivity of a particular substance. With this conclusion we agree. Furthermore, it is very likely that more than one mechanism is simultaneously present in PbS. The main reason for believing this is the wide variation in properties from one PbS film to another of similar preparation. One film may, for example, show a variation of conductivity with irradiance that is less rapid than linear, the next one may have a more rapid variation than linear, in a way strongly suggesting a superposition of mechanisms arising from details in the preparation beyond the control of the experimenter. However, a barrier theory seems capable of explaining many features of the experimental behavior, and since it was not considered by Rose in the general discussion quoted above, it seems worth developing here. We shall

compare the theory with experimental results on photoconductive films of high sensitivity obtained by Mahlman<sup>3</sup> and others, while on the staff of Electronics Corporation of America. I am grateful to Dr. Mahlman, to Professor W. B. Nottingham, and to others who have been connected with ECA, for valuable discussion.

### 2. DARK CONDUCTIVITY

One cannot hope to understand the photoconductivity of PbS films without having a good understanding of the conductivity of these films in the dark, and particularly of the variation of conductivity with preparation and with temperature. In Fig. 1 we show the logarithm of the conductivity as a function of  $10^3/T$ , where  $T$  is the absolute temperature, for a considerable number of films of a type actually used as photoconductors. These are chemically deposited films which differ in the amount of oxidation treatment which they have received. Unoxidized films show a high conductivity, varying only little with temperature. As the oxidation is increased, the resistance increases, particularly at the low temperatures, the curves showing a much steeper slope. Some films show a slope which approaches approximately a maximum value given by an exponential  $\exp(-\Delta E/kT)$ , where  $\Delta E$  is about 0.35 to 0.37 eV. Still further oxidation decreases the slope again, increasing the conductivity, until finally a highly oxidized film has a temperature dependence of conductivity much like an unoxidized film. Evaporated films treated directly with oxygen show similar characteristics, depending upon the amount of exposure to oxygen. The films of highest resistance are those which show the greatest photoconductivity. It has been shown by various workers<sup>4</sup> that the unoxidized films have the properties of  $n$ -type semiconductors, and that the properties change to those of  $p$ -type semiconductors as

\* This work was carried out as a consultant for the Electronics Corporation of America, and was supported by the U. S. Air Force.

<sup>1</sup> See, for instance, L. Sosnowski, *Phys. Rev.* **72**, 641 (1947); H. M. James, *Science* **110**, 254 (1949); E. S. Rittner, *Science* **111**, 685 (1950); R. A. Smith, *Phil. Mag.*, Suppl. **2**, 321 (1953); H. T. Minden, *J. Chem. Phys.* **23**, 1948 (1955).

<sup>2</sup> A. Rose, *Phys. Rev.* **97**, 322 (1955).

<sup>3</sup> G. W. Mahlman, *Phys. Rev.* **103**, 1619 (1956), preceding paper.

<sup>4</sup> For instance, H. Hintenburger, *Z. Physik* **119**, 1 (1942).

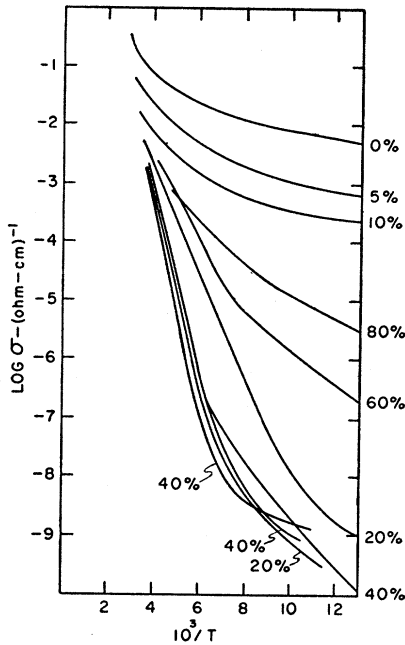


FIG. 1. Logarithm of conductivity vs  $10^3/T$ , for a number of experimental films (from G. W. Mahlman). The percentages indicate amount of oxidizing treatment, in arbitrary units. The films with highest photoconductive sensitivity are those with 20% to 40% oxidizing treatment.

we pass through the state of maximum resistance, and maximum photoconductivity.

Before seeking the interpretation of these facts in terms of the barrier theory, let us ask how the properties of the films compare with those of bulk PbS. A careful study of this material has recently been made by Petritz and Scanlon.<sup>5</sup> They have made measurements of the mobility of both holes and electrons as a function of temperature (both mobilities are approximately equal, and both vary approximately as  $T^{-5/2}$ ), and of the effective masses of holes and electrons (they estimate values of the effective mass of electrons varying from 0.22 to  $0.34m_e$ , where  $m_e$  is the electron mass, and for holes values from 0.1 to 0.36; since these estimates are not very certain, we adopt in the present calculations a value 0.30 for both holes and electrons). In Table I we give values for the mobility of either holes or electrons

TABLE I. Assumed mobilities of holes or electrons in PbS (from graph of Petritz and Scanlon).

$10^3/T$	$\mu$ (cm <sup>2</sup> /volt sec)
3	300
4	540
5	940
6	1300
7	1750
8	2300
9	2800
10	3400

<sup>5</sup> R. L. Petritz and W. W. Scanlon, Phys. Rev. **97**, 1627 (1955).

as a function of temperature, scaled off the graphs given by Petritz and Scanlon, and used as a basis of the calculations in this paper. Petritz and Scanlon also estimate the gap width as 0.37 ev. On the basis of these values we can compute the intrinsic conductivity of pure PbS by the equation

$$\sigma = \frac{2}{h^3} [(2\pi m^* kT)^{3/2} \exp(-\Delta E/2kT) e(\mu_+ + \mu_-)], \quad (1)$$

where  $m^*$  is the effective mass (assumed to be  $0.3m_e$  for both electrons and holes),  $\Delta E$  is the gap width 0.37 ev, and  $\mu_+$  and  $\mu_-$  are the mobilities of holes and electrons, assumed equal and taken from Table I.

In Fig. 2 we show the intrinsic conductivity so com-

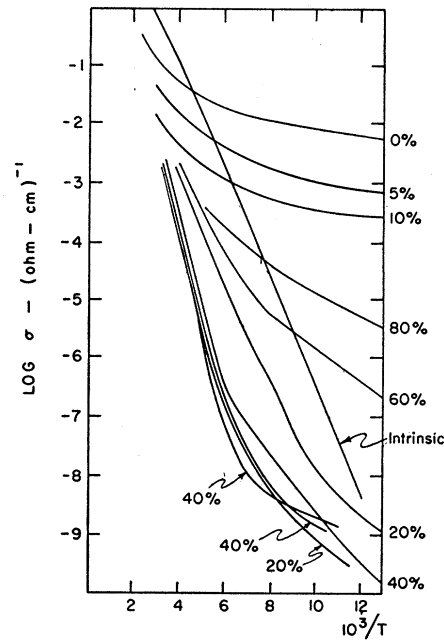


FIG. 2. Logarithm of conductivity vs  $10^3/T$ , for intrinsic PbS, computed from results of Petritz and Scanlon. The curves for the experimental films of Fig. 1 are included for comparison.

puted, and for comparison the conductivities of the same films shown in Fig. 1. It is at once obvious that some films have a much higher resistance than the intrinsic material. The slope of the intrinsic curve corresponds to the value  $\Delta E/2$ , where  $\Delta E$  is the experimental gap width of 0.37 ev, whereas the films of highest resistance have curves with a slope which empirically is very close to twice this value, or  $\Delta E$  rather than  $\Delta E/2$ . Our limiting films of high resistance are not, then, composed of intrinsic material. The greater slope of the conductivity curves for the films is, of course, the feature which results in the higher film resistance at low temperature.

It is well known that a material containing *n-p-n* junctions can have an effective resistance much higher

than that of intrinsic material. Let us see how barriers resulting from such junctions can very plausibly be present in the films, and how they can result in the observed conductivities.

First we have to know a few facts about the physical nature of the films. They are about  $0.2 \mu$  in thickness, and are seen under the electron microscope to consist of crystallites whose dimensions are about  $0.1 \mu$ , in contact. The unoxidized material, as we have stated, is  $n$  type, presumably on account of sulfur vacancies. We may now assume that the oxidizing treatment which changes the  $n$ -type material to  $p$ -type penetrates into the surfaces of separation between crystallites, in which the diffusion of the oxidizing agent would be rapid, and produces a thin layer of  $p$ -type material between the crystallites. Such a layer of  $p$ -type material between the  $n$ -type crystallites will produce  $n$ - $p$ - $n$  barriers of the required sort to result in a high resistance.

In Fig. 3 we show the way in which the energy bands will vary through such an  $n$ - $p$ - $n$  barrier, in three different cases of increasing thickness of  $p$ -type material (which presumably corresponds to increasing amounts of oxidation). We shall come later to the method of calculation of such curves. In Fig. 3(a) the layer is too thin to allow the development of a barrier of maximum height. In Fig. 3(b) the barrier is completely developed, and in Fig. 3(c) the layer of  $p$ -type material is so thick that there is not enough  $n$ -type material left to form a complete  $n$ -type barrier in the  $p$ -type material. We shall see later that all of these cases are likely to be met in practice, with the sizes of crystallites and probable concentration of impurities which we actually have.

We can now consider the expected behavior of the conductivity as a function of temperature for these three cases. In case (a) conductivity will take place largely by electrons which have enough energy to surmount the barriers in the thin  $p$ -type layers, so that the film will act like an  $n$ -type semiconductor. We may assume that the mobility of those electrons which can surmount the barrier is substantially the same as that of the electrons in the intrinsic material, and that the effect of the barriers is merely to reduce the number of electrons which can surmount them, and thus to carry current through the film. If  $\Delta E$  is the height of the top of the barrier above the Fermi level, the current will then have an exponential factor  $\exp(-\Delta E/kT)$ , and we see that  $\Delta E$  can be anything from a very small value (for the case where the barriers are not developed) up to  $0.37 \text{ ev}$  [when they are completely developed, as in case (b)]. Hence we may expect to find films whose conductivity curves show slopes anywhere from a small value to the value corresponding to  $0.37 \text{ ev}$ , or twice the slope of the intrinsic material. Films are observed with characteristics all through this range.

From the discussion just given, we see that the case (b), where the barriers are fully developed, will lead to a conductivity curve with slope corresponding to  $0.37 \text{ ev}$ , as is found experimentally for the films of

highest resistance. In this case conductivity will be produced both by holes and electrons, for now the holes just able to pass below the barriers marked " $n$ " in Fig. 3(b) in the valence band will be as plentiful as the electrons able to surmount the barriers marked " $p$ " in Fig. 3(b) in the conduction band. This is in agreement with the experimental fact that it is at this point of maximum resistance that the character of the conductivity changes from  $n$  type to  $p$  type. We also see clearly from this case why it is that such a model can lead to a much higher resistance than one has in the intrinsic material: current must be carried by minority carriers in both  $n$ -type and  $p$ -type regions (that is, in

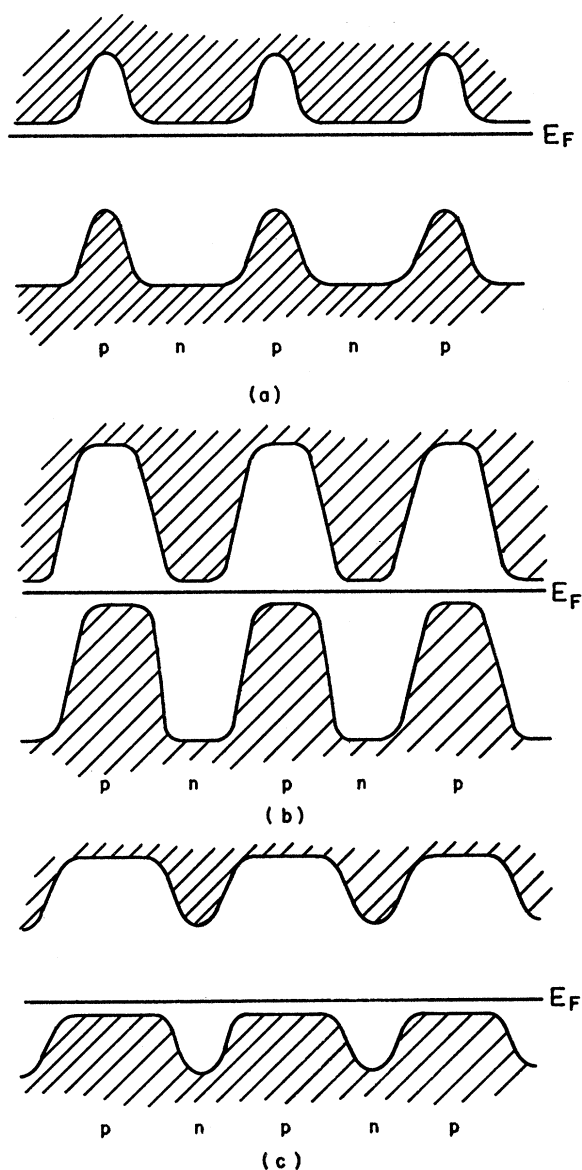


FIG. 3. Energy bands in barrier model of PbS. (a) Partially developed barriers, underoxidized case; (b) completely developed barriers; (c) partially developed barriers, overoxidized case.

the bulk of the crystallites and in the barriers), and these carriers are much less abundant than either holes or electrons would be in the intrinsic material.

As the material approaches case (c) of Fig. 3, the situation is the reverse of that shown in case (a), and most of the current will be carried by holes which can pass under the barriers remaining in the  $n$ -type regions, so that the conductivity will become  $p$ -type, and the resistance will decrease again. On account of the geometrical situation, however, we must expect a rather different behavior in this case from that found in case (a). It is clear that as  $p$ -type material is formed in more and more of the boundary layers between crystallites, it will be possible for this  $p$ -type material to join together into continuous paths through the crystal, which the current can traverse without having to go through the interior of the crystallites at all. Presumably such devious shunt paths for the current become rapidly more common, and furnish the main mechanism for carrying current in an overoxidized film.

We note, from Figs. 1 and 2, that while the curve for conductivity  $vs$   $10^3/T$  for an actual film may remain approximately straight through a number of powers of 10, still at very low temperatures the experimental curves all flatten out. The explanation for this is presumably to be found in the existence of some devious shunt paths through the crystal, of small cross-sectional area, but giving a small conductivity varying slowly with temperature, which is swamped by the main conductivity through the bulk of the material at high temperatures, but which becomes the principal form of conductivity at low temperatures. Such shunt paths could consist either of  $n$ -type regions in which the barriers were less fully developed than in the bulk of the material, or of  $p$ -type regions in which the conductivity of the boundary layers was so well developed that we had shunt paths through these boundary layers. It is found, by analysis of the experimental curves, that they can be well represented as a superposition of a principal conductivity behaving according to the barrier model of Figs. 3(a), 3(b), or 3(c), shunted by paths with much lower barriers, whose conductance at room temperature would be smaller than that of the main part of the film by a factor of something like  $10^6$ , but whose conductance would dominate at low temperatures. Since such shunt paths would be very erratic things, varying from film to film, it is likely that their existence is one of the major features leading to the observed variation in properties from one film to another.

We now have seen that the barrier theory can account for the general type of behavior observed in the dark conductivity. Let us next make these considerations more quantitative. First we consider the case of completely developed barriers as in Fig. 3(b). We have assumed in our qualitative discussion that the barriers were of height 0.37 eV, independent of temperature, so that the conductivity would contain a factor

$\exp(-\Delta E/kT)$ , where  $\Delta E$  has this value. It is obvious, however, that as the temperature goes up, the material, both  $n$  and  $p$  type, will tend to become intrinsic, the Fermi level assuming at high temperature a position in the middle of the gap, and the barriers will disappear. Let us inquire whether this will occur in the temperature range considered (the measurements on the films are at room temperature and below), and whether it will invalidate our argument leading to a straight-line curve for logarithm of conductivity  $vs$   $10^3/T$ . To answer this question we have calculated the way in which the Fermi level varies with temperature for various impurity concentrations, and have computed curves of conductivity  $vs$  temperature using the barrier model of Fig. 3(b), for these cases. It is well known that as the temperature goes up the Fermi level approaches the intrinsic value, more rapidly with low concentration of impurities than with high. Now, for reasons which we shall mention shortly, it seems necessary that the impurity concentration both in the  $n$ -type crystallites and the  $p$ -type surface layers must be at least of the order of magnitude of  $10^{18}$  per cc. It is reasonable that we should actually have such numbers of impurity centers. Thus, Petritz and Scanlon<sup>5</sup> quote impurity concentrations in synthetic single crystals, and these come out several times  $10^{18}$ .

We now find that for impurity concentrations of  $10^{18}$  or greater, the variation of the Fermi level with temperature is not enough, in the range of temperatures used, to affect our arguments. Specifically, in Fig. 4 we show the conductivity  $vs$  temperature for a model like

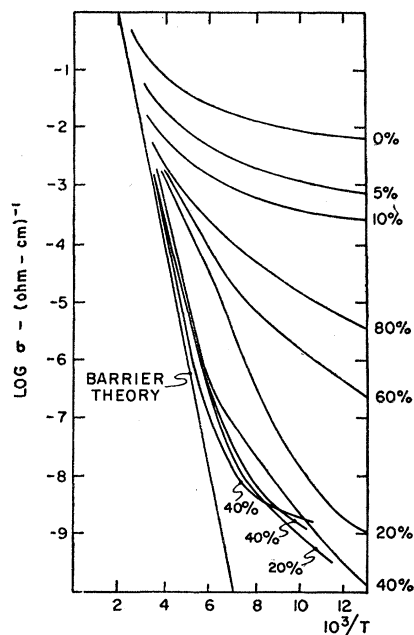


FIG. 4. Logarithm of conductivity  $vs$   $10^3/T$ , for the barrier model of Fig. 3(b), assuming  $10^{18}$  impurity atoms/cc in both  $n$ - and  $p$ -type material. The curves for the experimental films of Fig. 1 are included for comparison.

that of Fig. 3(b), assuming  $10^{18}$  impurity centers per cc in both *n*- and *p*-type regions, and taking account of the variation of the Fermi level with temperature. For comparison we show the same experimental curves which we have given in Figs. 1 and 2. It is clear from this figure that this theoretical curve represents very well the limiting form which the experimental curves approach, for the films of highest resistance. Calculated curves corresponding to impurity concentrations greater than  $10^{18}$  are practically indistinguishable from that shown in Fig. 4.

We shall next discuss the cases of incompletely developed barriers, as shown in Figs. 3(a) and (c); our discussion will apply specifically to case (a), but that of (c) is entirely parallel. We shall first use a simple and approximate method of discussion, then a more sophisticated and correct method, both of which lead to substantially the same answers. In Fig. 5 we show the top of the valence band and the bottom of the conduction band as a function of position through the barrier. We assume that *n*-type material with a density of  $N_0$  donors per unit volume persists up to a dividing line shown and that *p*-type material with a density of  $N_0$  acceptors per unit volume (we take the donor and acceptor densities as being equal for convenience and for lack of knowledge to the contrary), is present in the barrier. In the *n*-type region we let  $E(x)$  be the energy of the bottom of the conduction band, measured upward from the Fermi level, and in the *p*-type region we let  $E(x)$  be the top of the valence band, measured downward from the Fermi level (so that  $E(x)$  is positive in both cases). We assume that  $E(x)$  is measured in electron volts; that is, it is  $e$  times an electrostatic potential in volts. We let  $E_0$  be the height of the bottom of the conduction band in the *n*-type region above the Fermi level, or the distance of the top of the valence band in the *p*-type region below the Fermi level, in the case of infinitely wide regions of *n*-type and *p*-type material; that is, in the case of the fully developed barriers of Fig. 3(b).

Now we consider the curved parts of the curves of  $E(x)$  as shown in Fig. 5. The curvature arises from the volume density of positive charge in the depletion layer in the *n*-type region, and of negative charge in the depletion layer in the *p*-type region. For the simplified theory which we shall first use, we assume that the depletion is complete; that is, that the charge density, positive or negative as the case may be, is constant, equal to that of  $\pm N_0$  electronic charges per unit volume. In such a case Poisson's equation as applied to either *n*- or *p*-type regions becomes

$$d^2E/dx^2 = N_0e^2/k\epsilon_0, \tag{2}$$

where  $x$  is the distance measured perpendicular to the barrier,  $e$  is the magnitude of the electronic charge,  $k$  is the dielectric constant (assumed to be 17.9 for PbS), and  $\epsilon_0 = 8.85 \times 10^{-12}$  farads/meter, if we use mks

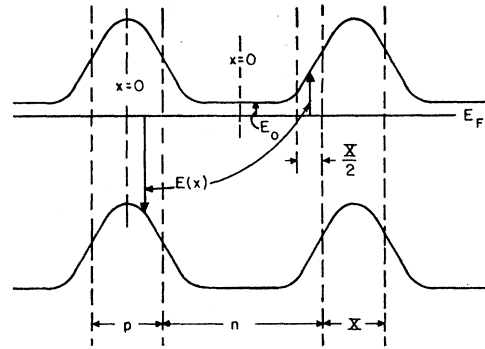


FIG. 5. Valence and conduction bands in case of Fig. 3(a), showing notation used in text.

units. A solution of Eq. (2) is

$$E = \text{const} + \frac{1}{2} \frac{N_0e^2}{k\epsilon_0} (x - \text{const})^2. \tag{3}$$

We are to set up similar solutions in both *n*-type and *p*-type regions which must join with constant value and constant slope at the boundary between the two regions.

The boundary conditions are different in the *n*-type and the *p*-type regions for the case we are considering. Let  $X$  be the thickness of the *p*-type region. In the *p*-type region the parabolic behavior of the  $E$  vs  $x$  curve will start at the center of the region. Hence the value of  $E$  at the edge of the *p*-type region will be

$$E = \text{const} + \frac{1}{2} \frac{N_0e^2}{k\epsilon_0} \left(\frac{X}{2}\right)^2. \tag{4}$$

The slope of the curve at this point must be equal to the slope of the corresponding curve in the *n*-type region, which means that the thickness of the depletion layer in the *n*-type region must be  $X/2$ , equal to half the width of the *p*-type region, so that the total amount of charge in the barrier, made up of positive charge in the *n*-type region, negative in the *p*-type region, will be zero. Then the value of  $E(x)$  in the *n*-type region, at the boundary between *n*-type and *p*-type regions, will be  $E_0 + (N_0e^2/2k\epsilon_0)(X/2)^2$ . The height of the barrier, in the *p*-type region, above the Fermi level, will then be

$$\begin{aligned} \text{barrier height} &= E_0 + 2(N_0e^2/2k\epsilon_0)(X/2)^2 \\ &= E_0 + (N_0e^2/4k\epsilon_0)X^2. \end{aligned} \tag{5}$$

If we let  $N_0 = 10^{18}/\text{cc}$ , the quantity  $(N_0e^2/4k\epsilon_0)X^2$  will equal 0.37 eV for  $X = 382$  angstroms. In other words, for a *p*-type region of this thickness, and for a low temperature where  $E_0$  is negligible, the barrier will just become complete, while for any smaller thickness we have a barrier such as is shown in Fig. 3(a), of less than the maximum height. For other values of  $N_0$  the critical thickness of the *p*-type region for giving a barrier of maximum height will be proportional to  $N_0^{-1/2}$ .

We can now see why it was stated earlier that the

density of impurity centers,  $N_0$ , cannot be much less than  $10^{18}$ . For let us remember that the assumed thickness of a crystallite is about  $0.1 \mu = 1000$  A. With  $N_0 = 10^{18}$ , we have just seen that the critical thickness of the  $p$ -type region for development of complete barriers is 382 A. In such a case the  $n$ -type region left between two successive  $p$ -type regions will be  $1000 - 382 = 618$  A. But if the value of  $N_0$  were much less, so that the thickness of the  $p$ -type region were much greater than 382 A, the thickness of the  $n$ -type region would be correspondingly less, and it would be perfectly possible to have values such that a complete barrier could not build up in either the  $n$ -type or the  $p$ -type region. In fact, the critical concentration is that for which the thickness of the  $p$ -type region, for complete barrier formation, is 500 A, and we see at once that this is  $(382/500)^3 10^{18} = 8.8 \times 10^{17}/\text{cc}$ . For impurity concentrations less than this value, complete barrier height cannot be built up.

We see, then, that according to this elementary treatment, for an impurity concentration of  $10^{18}/\text{cc}$ , the barrier height will build up proportionally to the square of the thickness of the  $p$ -type region, to a limiting value of 0.37 ev, which it will reach at a thickness of 382 A. As the  $p$ -type region becomes thicker we shall continue to have these barriers of maximum height, until the thickness of the  $n$ -type region is reduced to 382 A, after which the barrier height in the  $n$ -type region will decrease proportionally to the square of the thickness of the  $n$ -type region. The first situation, where the barrier height is proportional to the thickness of  $p$ -type region, is that shown in Fig. 3(a); the second situation, with maximum barrier height, is that of Fig. 3(b); the third is that of Fig. 3(c). The region of tolerance over which the case of maximum carrier height exists is larger, the higher the impurity concentration. In the range of concentrations which we may well expect—a small multiple of  $10^{18}$ —we see that there is appreciable tolerance, so that films of maximum resistance would be expected to occur in substantial number, which agrees with the observations.

Now we shall discuss this same problem of the formation of barriers from a more sophisticated point of view. The positive charge density in the  $n$ -type region, and the negative density in the  $p$ -type region, are not really those arising from  $\pm N_0$  electronic charges per unit volume, unless the conduction band lies so far above the Fermi level in the  $n$ -type region that the impurity levels are entirely empty, or the valence band lies so far below the Fermi level in the  $p$ -type region that the acceptor levels are entirely filled with electrons. More generally, we can compute the positive charge density in the  $n$ -type region from the following formula for  $N$ , the number of positive charges per unit volume, with a similar formula for the  $p$ -type region:

$$N = N_0 - N_0 / \{ \exp[(E - E_1)/kT] + 1 \} - (2/h^3)(2\pi m^* kT)^{3/2} / [\exp(E/kT) + 1]. \quad (6)$$

In Eq. (6) the first term  $N_0$  stands for the number of donors per unit volume. The second term represents the number of donors which contain electrons, and hence do not contribute to the net positive charge density; the quantity  $E_1$  measures the distance of the donor level below the bottom of the conduction band. The third term represents the number of electrons per unit volume in the conduction band, which therefore must be subtracted from the number of positive charges per unit volume. The expression (6) is such that if  $E = E_0$ , the number  $N$  is zero; that is,  $E_0$ , as assumed earlier, represents the bottom of the conduction band (measured up from the Fermi level) in a case of an infinite sample of material, in which the charge density must be zero.

To obtain a rigorous solution of the problem of finding  $E(x)$  through the barrier, we must rewrite Poisson's equation, Eq. (2), replacing  $N_0$  which appears in Eq. (2) by  $N$  as given in Eq. (6). When we do this we note immediately that if  $E = E_0$ , so that  $N = 0$ , we have a solution corresponding to constant  $E$ , the ordinary case of an infinite sample of material. We are interested, however, in the case of finite thicknesses of material, corresponding to the barriers, so that we must integrate the whole differential equation, which is a differential equation of a complicated form for  $E$  as a function of  $x$ . This can only be handled by numerical integration, and the writer has carried out numerical integrations for the necessary cases, assuming  $N_0 = 10^{18}/\text{cc}$ , and assuming  $E_1 = 0.01$  ev. We shall now discuss the general nature of these solutions.

Since we have a second-order differential equation, there will be two arbitrary constants. We note by symmetry from Fig. 3 or Fig. 5 that  $E$  will have a minimum at the mid-point of the  $n$ -type region, or at the mid-point of the  $p$ -type region. Let us then measure our coordinate  $x$  from this mid-point and choose one of the two arbitrary constants by requiring that the slope  $dE/dx$  be zero at this point. Then there will be a solution corresponding to each value of  $E$  at  $x = 0$ . For  $E = E_0$  the curve will be a horizontal straight line. For larger initial  $E$  the curve will start to rise as  $x$  increases, and by the time it has risen an amount of the order of magnitude of  $kT$ , the function  $N$  of Eq. (6) will become substantially equal to  $N_0$ , and the curve will be parabolic, of the form given in Eq. (3), with appropriate constants. In our numerical integration it has been convenient to carry each curve out to large enough values of  $E$  so that this parabolic approximation is justified, and then to evaluate the two constants as functions of the ordinate of the curve at  $x = 0$ . For better understanding we show in Fig. 6 a family of such curves.

We must now use one such curve for the  $n$ -type region and another for the  $p$ -type region, subject to two conditions: the function must be continuous, and the slope must be continuous, at the boundary between the two regions. These conditions can be satisfied by

numerical methods which we shall not go into. When we satisfy these boundary conditions we find the exact shape of the barrier and we find the barrier height as a function of the thickness of the *p*-type region, replacing the simple value of Eq. (5). As far as the shape of the barrier is concerned, the departure from the parabolic form given in the elementary discussion is unimportant. As far as the height is concerned, we exhibit some of the exact results in Figs. 7 and 8. In Fig. 7 we show the barrier height as a function of *X* for  $10^3/T=8$ , as calculated by this rigorous method. For comparison we give the parabola given by Eq. (5). We see that there is substantial agreement between the parabola of Eq. (5) and the rigorous curve for values of *X* less than the

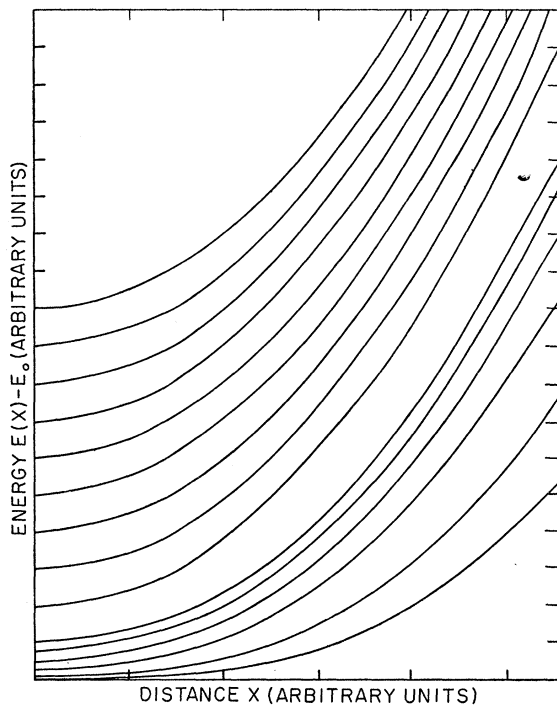


FIG. 6.  $E(x) - E_0$  vs *x*, both expressed in suitably chosen dimensionless units, from Poisson's equation derived by combining Eqs. (2) and (6), for a number of initial conditions.

critical value for formation of the complete barrier, and above the critical value the barrier height stays approximately constant; the only real difference between the exact solution and the approximation is that in the exact case there is a smooth transition from one case to the other.

In Fig. 8 we show the barrier heights for a number of values of *X* as a function of  $10^3/T$ . These variations include all of the temperature dependences found in Eq. (6), including the variation of the quantity  $E_0$  with temperature, the height of the bottom of the conduction band above the Fermi level. We see that for values of  $10^3/T$  greater than 4, which includes the cases met in practice with the photoconductive measurements, the

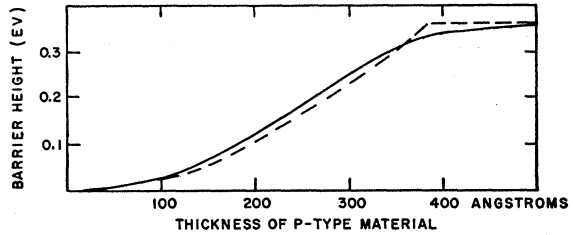


FIG. 7. Barrier height as a function of *X*, thickness of *p*-type layer, for  $10^3/T=8$ ,  $10^{18}$  impurity atoms/cc. Dashed curve, parabola and constant value given by elementary treatment.

variation of barrier height with temperature is unimportant. We thus justify the qualitative discussion which we have given earlier: in cases of only partially developed barriers the curve of logarithm of conductivity vs  $10^3/T$  will be approximately a straight line whose slope depends on the height of the barriers, and the maximum such slope corresponds to completely formed barriers, for which the slope corresponds to 0.37 eV. In this way we explain the fact that films are observed corresponding to many different slopes, up to a maximum value. When we actually compute curves of conductivity for barriers of various heights we find good agreement between them and various films in the straight-line portion of the experimental graphs; as we have stated earlier, the tendency to flatten out at low temperatures, found in all experimental curves, must be explained by devious shunt paths of low-resistance material whose conductivity does not vary greatly with temperature, and since this is a random situation we cannot set up any single theoretical curve to agree with experiment in this region.

3. MECHANISM OF PHOTOCONDUCTIVITY

In the preceding section we have seen that the barrier theory is capable of explaining the general features of the dark conductivity of the PbS films. Now we inquire how photoconductivity is to be explained. When light is absorbed anywhere in the crystal, whether in the *n*- or *p*-type regions, an electron will be raised to the conduction band, leaving a hole in the valence band. Any radiation whose wavelength is shorter than that corresponding to the gap width of 0.37 eV can cause formation of electron-hole pairs, and it is well known that this wavelength agrees well with the long-wave

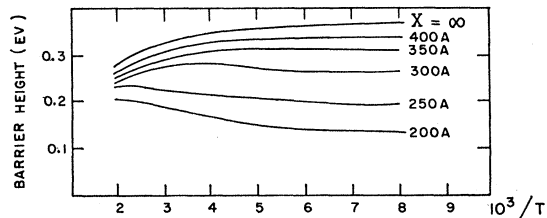


FIG. 8. Barrier height as a function of  $10^3/T$ , for a number of values of *X*, thickness of *p*-type layer, assuming  $10^{18}$  impurity atoms/cc.

limit of infrared sensitivity of PbS photoconductors. The electron so introduced into the conduction band will now tend to fall to the lowest possible energy, or into an  $n$ -type region, whether it originates in an  $n$ -type or a  $p$ -type region, and the hole will in a similar way find its way into a  $p$ -type region. The presence of extra electrons in the  $n$ -type region, extra holes in the  $p$ -type region, will neutralize some of the space charge producing the barriers. Thus the barriers will be lowered, and the conductivity will correspondingly be increased. Let us now put these ideas in more quantitative language.

There are two aspects to the problem, the lowering of the barrier by the hole-electron pairs, and the calculation of the number of such pairs produced by the irradiation. Let us consider first the lowering of the barriers. Let us assume that we have on the average  $n$  hole-electron pairs per unit volume, produced by irradiation. Now the electrons, in the  $n$ -type regions, will tend to drift to the interface between the depletion layer and the neutral material, and the holes in the  $p$ -type regions will drift to the surface of the depletion layer in that region; that is, if the barriers are incompletely developed, they will be located in the center of the  $p$ -type region. They will neutralize part of the charge in the depletion layers, and will have the effect of decreasing the effective thickness of those layers, hence decreasing the barrier height; we may use our elementary theory to find the decrease of barrier height from Eq. (5). Let the dimension of a crystallite be  $D$  (we shall assume it to be  $0.1 \mu$ ). The electrons in a crystallite will be distributed over two interfaces between neutral regions and depletion layers. Hence the charge per unit area on either of these interfaces will be  $-neD/2$ . This will neutralize volume charge whose charge density in the depletion layer is  $N_0e$ . Therefore it will neutralize volume charge extending to a depth  $nD/2N_0$ . Now the combined thickness of the depletion layers in  $n$ - and  $p$ -type regions, from the center of the  $p$ -type region to the interface in the  $n$ -type region, in the absence of irradiation, is  $X$ . Hence in the presence of irradiation it will be reduced to  $X - nD/N_0$ , reduced by the amount of the regions neutralized in both depletion layers. We therefore conclude that the barrier height in the presence of radiation will be given by

$$\text{barrier height} = E_0 + (N_0e^2/4k\epsilon_0)(X - nD/N_0)^2, \quad (7)$$

which follows at once from Eq. (5).

From the barrier height, as found in Eq. (7), we can immediately deduce the conductivity. The conductivity will depend on barrier height through the exponential  $\exp[-(\text{barrier height})/kT]$ , so that  $\ln\sigma$  will be proportional to  $-(\text{barrier height})/kT$ . We let  $\sigma_L$  be the conductivity in the presence of light [for which we use Eq. (7)], and  $\sigma_D$  be the conductivity in the dark, for which  $n=0$ , and we let

$$(N_0e^2/4k\epsilon_0)X^2 = \Delta E_0, \quad (8)$$

so that  $E_0 + \Delta E_0$  is the barrier height in the dark (ordinarily  $E_0$  is small enough to disregard). Then we find

$$\ln\left(\frac{\sigma_L}{\sigma_D}\right) = \frac{\Delta E_0}{kT} \left( \frac{2nD}{N_0X} - \frac{n^2D^2}{N_0^2X^2} \right). \quad (9)$$

In Eq. (9) we see the way in which the conductivity varies with  $n$ . If we solve the quadratic (9) for  $nD/N_0X$ , we find

$$nD/N_0X = 1 - [1 - (kT/\Delta E_0) \ln(\sigma_L/\sigma_D)]^{1/2}. \quad (10)$$

Equation (10) is particularly interesting, for it allows us to solve for  $nD/N_0X$ , the fractional decrease in the barrier thickness produced by radiation, in terms of known quantities. To find it, we must know  $\Delta E_0$ , which we get from the slope of the experimental curve of conductivity  $vs 10^3/T$  (disregarding  $E_0$ ), and the dark conductivity. In this latter quantity, if we are working at low temperatures where the experimental curve of dark conductivity  $vs$  reciprocal temperature has flattened off, we use an extrapolated dark conductivity corresponding to constant barrier height, or a straight-line extrapolation; for we assume that the flattening off is a result of shunting by devious paths which do not contribute to the photoconductivity, and we wish to subtract the conductivity arising from these devious paths. When we carry through such calculations in actual cases, we find that in the experiments to be described, the barrier has been reduced in thickness by some 30% by the most intense irradiation employed.

The second part of our problem is to find the way in which  $n$ , the number of electron-hole pairs per unit volume, depends on the irradiance  $I$ . In the first place, the number of such pairs created per unit time will be proportional to  $I$ ; let it be called  $aI$ . The constant  $a$  will be determined by the fact that some fraction of all photons striking the film will produce pairs. The fraction will be less than unity because some of the incident radiation will be reflected or scattered, and some will travel through without being absorbed. In a steady state, the number of electron-hole pairs created per unit time will be balanced by the number recombining again. We must consider the possible mechanisms for this recombination. Since an electron and hole, after their creation, migrate in opposite directions, and come to rest at opposite sides of a barrier, separated by several hundred angstroms, a direct recombination is hardly possible. We are much more likely to have recombination by an indirect process. An electron, trapped in an  $n$ -type region, will recombine with a hole which happens to be found in its neighborhood, or a hole, trapped in a  $p$ -type region, will recombine with an electron which happens to be in its neighborhood. Let us consider these possibilities more in detail.

Suppose that we have the case of incompletely developed barriers, as shown in Fig. 3(a). Then current will be carried largely by electrons surmounting the



barriers in the  $p$ -type regions. These electrons can combine with holes trapped in the  $p$ -type region. The number of such recombinations per unit time will be proportional to  $n$ , the number of trapped holes; and to the number of electrons per unit volume in the  $p$ -type region. Since these are the same electrons which are carrying the current, the number of recombinations per unit time will be proportional to  $n\sigma$ . Every time an electron recombines with a hole trapped in a  $p$ -type region, it must leave behind a hole in the  $n$ -type region. Hence effectively it is neutralizing one of the electrons trapped in the  $n$ -type region. Similar considerations will hold in the cases shown in Figs. 3(b) and 3(c).

Combining these two mechanisms, then, we must have

$$\frac{dn}{dt} = aI - \frac{n}{\tau}, \quad (11)$$

where the time constant  $\tau$  is inversely proportional to the conductivity, so that

$$\sigma\tau = A. \quad (12)$$

Since the time constant depends on conductivity, it really depends on  $n$ , so that Eq. (11) is more complicated than it seems at first sight. We shall use Eq. (11) in Sec. 4 to discuss transient effects, but at the moment we are interested in the steady state. Here we have

$$n = aI\tau. \quad (13)$$

We may now combine Eqs. (10), (12), and (13), noting that  $\sigma$  appearing in Eq. (12) is the same as  $\sigma_L$  appearing in Eq. (10), and obtain

$$(aAD/N_0X)I = \sigma_L \{1 - [1 - (kT/\Delta E_0) \ln(\sigma_L/\sigma_D)]^{-1/2}\}. \quad (14)$$

In Eq. (14) we have an expression for the irradiance as a function of the conductivity, and if we plot the curve with  $I$  as abscissa,  $\sigma_L$  as ordinate, we find the conductivity as a function of irradiance.

We are now ready to start comparison of some of these results with experiment, though we shall have to postpone some comparisons until later, when we discuss the time variation more in detail. First we consider some of the experimental results. In Fig. 9 we show the logarithm of the conductivity of a typical film vs  $10^3/T$ , for various irradiances. In Fig. 10 we show results for the logarithm of the time constant as a function of  $10^3/T$ , and for comparison the logarithm of the conductivity, in the dark and for a fixed irradiance, for several typical films.

The first observation which we make from Fig. 10 is that in a qualitative way the inverse proportionality between conductivity and time constant, postulated in Eq. (12), certainly holds. The time constant decreases in going to higher temperature, or to higher irradiance, in much the same way in which the conductivity increases. For some films the relation given in Eq. (12)

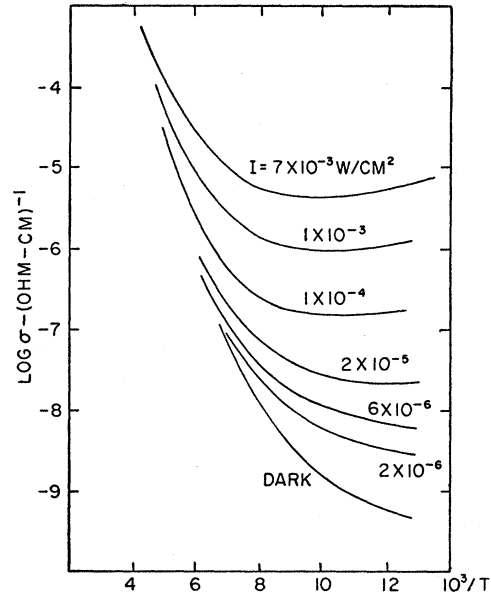


FIG. 9. Logarithm of conductivity vs  $10^3/T$ , for various irradiances, observed for film R19X.

seems to be almost quantitatively fulfilled, but for others it is only approximate. The tendency is for the measured time constant to vary considerably less than the conductivity, both with temperature and with irradiance. This appearance may be partly a result of inadequacies in the experimental technique. The time constant was very hard to measure accurately at the low temperatures and low irradiances, because the resistance of the films was so extremely high, and the expected direction of the errors would lead to a true time constant much longer than the measured value. More accurate measurements, carried out in a few cases, gave a much longer time constant for the high-resistance cases, and more nearly reciprocal relations, as postulated in Eq. (12), than is indicated in the results of Fig. 10. In making this comparison, one must take account of a correction to the measured time constant discussed in Sec. 4; this correction was not made in the results of Fig. 10, which represent the direct experimental data.

It seems reasonable, then, as a first approximation, to assume the correctness of Eq. (12). One point should be noted in connection with this equation, in the case of low temperatures, where the curve of conductivity vs temperature flattens out. We find experimentally that the curve of time constant flattens out in a similar way. This would imply that the shunt-path conductivity, which we have assumed to be responsible for the conductivity at low temperature and low irradiance, should at the same time supply an electron concentration which would be effective in producing recombinations with trapped holes in the  $p$ -type regions. This perhaps could happen if the shunt paths were really very minute, but distributed widely throughout the

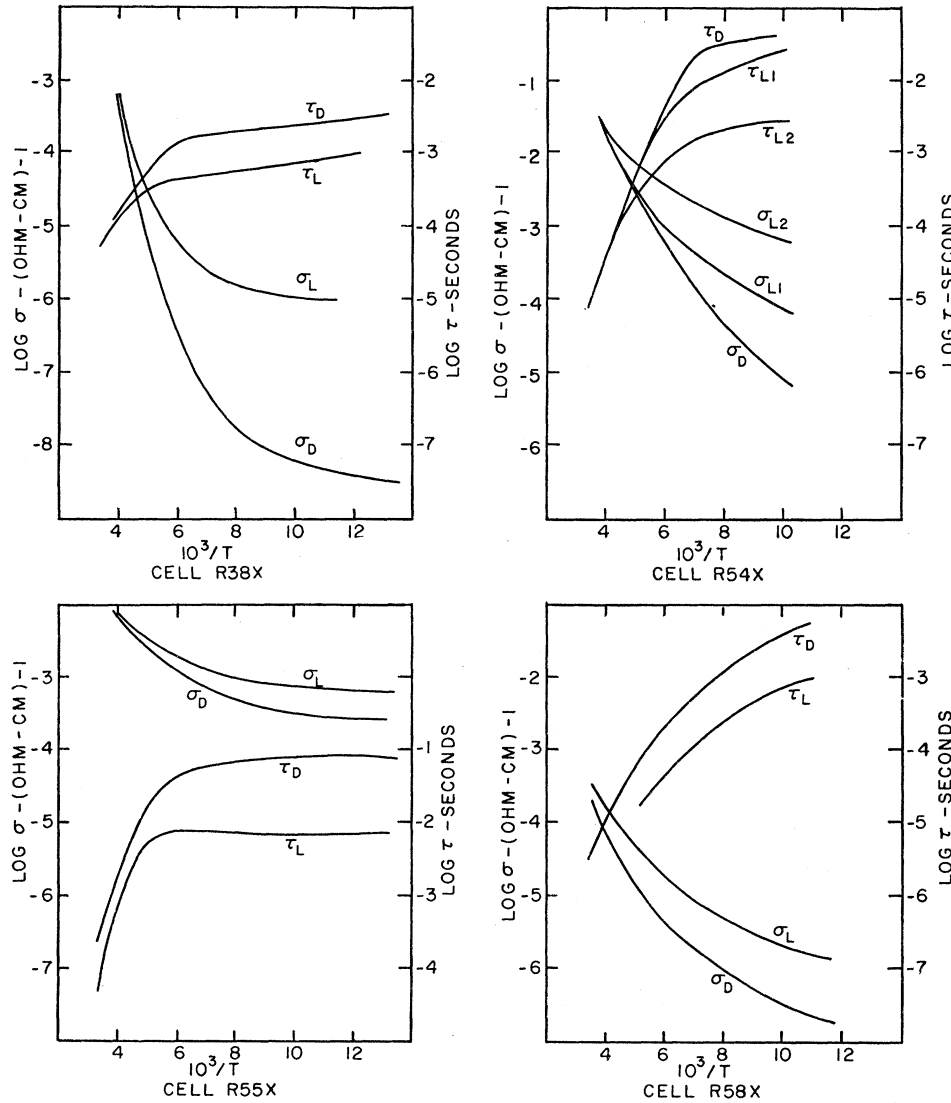


FIG. 10. Logarithm of time constant and of conductivity vs  $10^3/T$ , for various films both in the dark ( $D$ ) and at fixed irradiance ( $L$ ).

body of the material, consisting really of randomly scattered regions of lower than average barriers. In such a case electrons carrying current in the shunt paths might be found close enough to the barriers in question to produce recombinations with trapped holes. It must be admitted that this view is somewhat unclear, however, and that this furnishes one of the weak points of the theory. However, whatever may be the mechanism of the recombination, an equation of the form of Eq. (11) seems most likely to be true, and the same time constant which is directly measured by the experiments to be discussed in Sec. 4 should be the one appearing in Eq. (13). In other words, by using measured time constants in Eq. (14), writing it in the form

$$(aD/N_0X)I = (1/\tau_L)\{1 - [1 - (kT/\Delta E_0) \times \ln(\sigma_L/\sigma_D)]^{-1}\}, \quad (15)$$

we should have a relation making no use of the assumed

relation between time constant and conductivity, and hence based on somewhat firmer ground.

Now let us make some comparison between our theory of photoconductivity and experiment. In the first place, we show in Fig. 11 a curve of conductivity vs irradiance, for a typical case, computed from Eq. (14). This curve, which is plotted on a logarithmic scale, shows a somewhat less rapid variation than linear of conductivity as a function of irradiance, continuing without great change in slope up to a limiting irradiance where the barriers disappear. The slope of the curve depends on the value of  $kT/\Delta E_0$ , but corresponds in most cases to a dependence of  $\sigma_L$  on a power of  $I$  between 0.7 and 0.95. The experimental curves for conductivity vs irradiance mostly have this general form, though as we have stated earlier, they can vary much more erratically than the theory would suggest, in some cases even being more rapid than linear.

In this connection, we may note that if we use Eq. (15) instead of the more specialized form [Eq. (14)], we can ask how the conductivity would vary with irradiance if the time constant were not inversely proportional to the conductivity. As an extreme case, if  $\tau_L$  were independent of conductivity or irradiance, Eq. (15) would lead to a very strong dependence of conductivity on irradiance. For small irradiances, where we can expand the square root in Eq. (15) in power series, we should find

$$(\sigma_L/\sigma_D) = \exp(2aD\tau_L\Delta E_0I/N_0XkT), \quad (16)$$

an exponential dependence on  $I$ , if  $\tau_L$  were independent of  $I$ . We may therefore plausibly suppose that the observed strong variation in occasional films arises from a time constant which varies somewhat less rapidly with conductivity than Eq. (12) would demand. The fact that most of the observed curves show a variation which is less rapid than linear, however, and qualitatively similar to that of Fig. 11, would indicate that our assumed inverse relationship between time constant and conductivity is actually well justified.

If we assume the correctness of Eq. (12) and assume furthermore that the constant  $A$  is independent of temperature (which is not exactly true, as we shall see

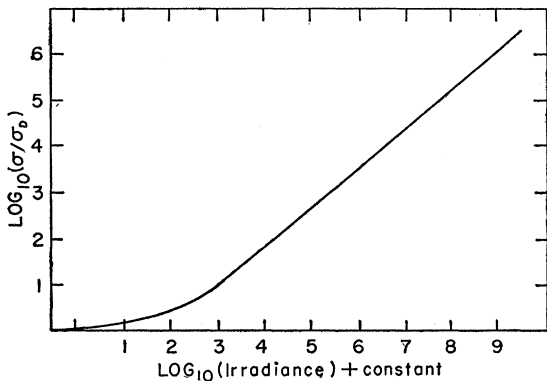


FIG. 11. Logarithm of conductivity vs logarithm of irradiance, for a typical case, computed by Eq. (14). The curve stops abruptly as indicated, at the point where the barriers are reduced to zero.

later), then Eq. (14) would give us a complete framework for calculating the conductivity as a function of irradiance at any temperature. To a first approximation, this simple assumption works surprisingly well. Thus, in Fig. 12, we show calculated curves for conductivity as a function of reciprocal temperature, for various irradiances, for the same film whose conductivity was plotted in Fig. 9, compared with the observed points. In making this calculation, we have taken for  $\sigma_D$  an assumed value corresponding to a straight-line extrapolation of the conductivity vs  $10^3/T$  curve, and then have added the conductivity of the shunt paths to the calculated  $\sigma$ . This seems to be the most reasonable way to correct for these shunt paths. We have furthermore chosen a single value of the quantity  $(aAD/N_0X)$ ,

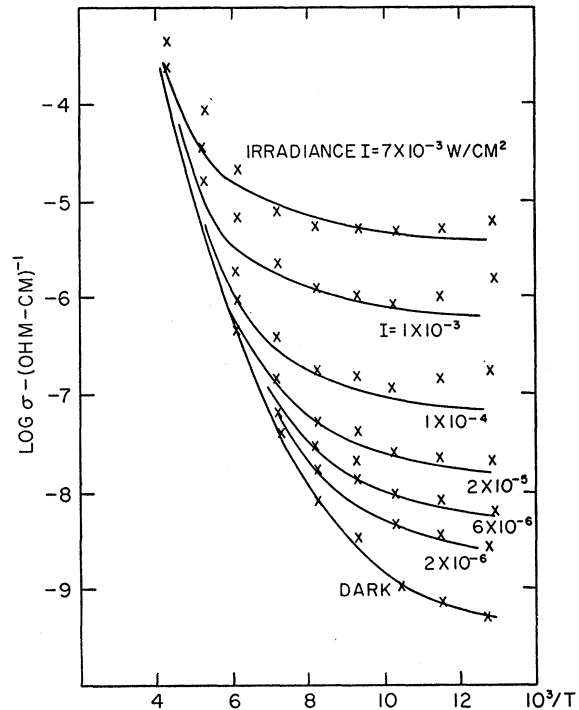


FIG. 12. Logarithm of conductivity vs  $10^3/T$ , for various irradiances, for film R19X, calculated on assumption that  $A$  is independent of temperature. Experimental points shown by crosses.

regarded as a disposable parameter, to fit the curves most accurately. It is obvious that we have in this way an explanation of the general form of the observed curves.

We can improve the agreement by taking account of the fact that Eq. (12) with  $A$  independent of temperature, does not agree very well with experiment. In the case of the film which we are using as an example, we do not have good data for the dependence of time constant on its dependence on temperature at one fixed irradiance. In Fig. 13 we show the values of  $\sigma_L\tau_L$  observed as a function of temperature (making the corrections to be discussed in Sec. 4), for an irradiance of about  $1 \times 10^{-4}$  w/cm<sup>2</sup>. We see that this quantity

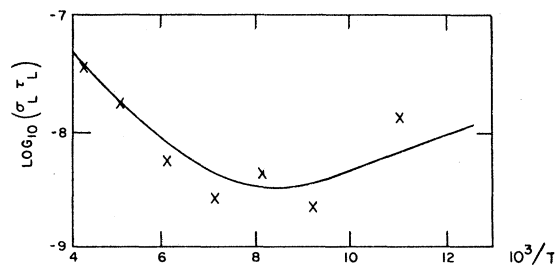


FIG. 13. Quantity  $\sigma_L\tau_L = A$  (plotted logarithmically) as function of  $10^3/T$ , for film R19X, at irradiance of  $1 \times 10^{-4}$  w/cm<sup>2</sup>. Crosses show experimental points; curve is best estimate of experimental value deduced from the observed points.

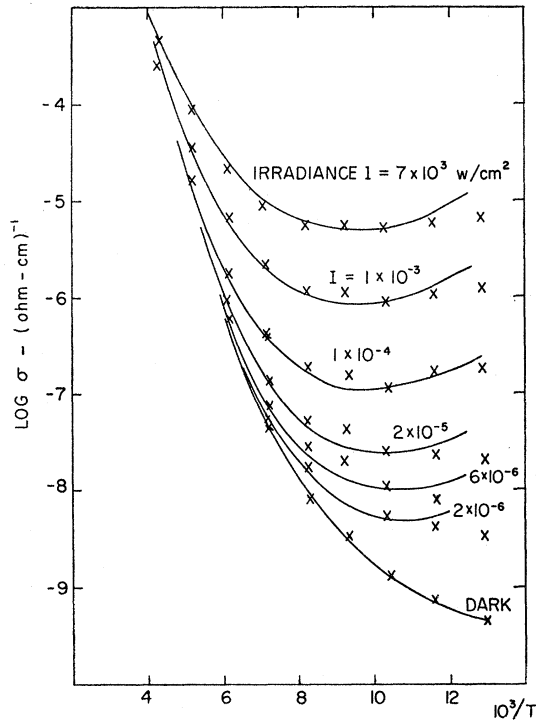


FIG. 14. Logarithm of conductivity vs  $10^3/T$ , for various irradiances, for film R19X, calculated on assumption that  $A$  varies with temperature as given by smoothed curve of Fig. 13. Experimental points shown by crosses.

varies by over a factor of ten from low to high temperature. If we use a value  $A(T)$  determined from Fig. 13, but still assume that Eq. (12) holds for each temperature, we find calculated curves for conductivity vs  $10^3/T$  at different irradiances as shown in Fig. 14. It is clear that this has improved the agreement between theory and experiment, as compared with Fig. 12.

It seems, then, that our explanation is capable of describing the general nature of the dependence of conductivity on irradiance with satisfactory accuracy. The film which we have used as an illustration is a fairly standard one, and similar calculations on other films give comparable results. We shall now proceed in the next section to discuss further details of the measurement of the time constant and then the numerical values of the various constants entering into the calculations.

#### 4. TRANSIENT EFFECTS AND THE MEASUREMENT OF TIME CONSTANT

In Eq. (11) we have the equation for transient effects. This equation is more complicated than it seems, because of the dependence of the time constant on the conductivity. Thus if we excited the film with a high irradiance, and then suddenly turned off the illumination, we should initially have a high value of  $n$ , and a large conductivity, with a consequent short time constant. We should expect initially a rapid decay, but

then as the conductivity became smaller, the time constant would increase, and the later part of the decay would be much slower. Such behavior has been shown in experimental curves of the decay from a high initial excitation. As a result of this effect, the direct measurement of time constant is more complicated than would appear at first sight.

Two experimental methods have been used for determining the time constant. One, of which very little use was made, is based on the experiment described in the preceding paragraph. Most of the measurements, however, were made by superposing a constant irradiance, and an additional square-wave-modulated irradiance, of such an amount that the conductivity increased by no more than five percent of the constant value. When this additional square-wave pulse stops, the conductivity decays from the steady-state value characteristic of the added irradiance, to that characteristic of the steady irradiance. This decay is very approximately exponential, and  $\tau$  is closely related to the time constant of the exponential decay. We shall now prove this fact, and discuss the method.

Let  $\sigma_L$  be the conductivity characteristic of the steady irradiance, and let  $n_L$  be the associated value of  $n$ , related to it by Eq. (9) or (10). Let  $\tau_L$  be the value of  $\tau$  connected with this value  $n_L$ . Now we consider the decay indicated by Eq. (11), when we start at  $t=0$  with a value of  $n$  somewhat greater than  $n_L$ , and let it decay down to  $n_L$  subject to the irradiance connected with the subscript  $L$ . From Eq. (13), we have

$$n_L = aI\tau_L. \quad (17)$$

Then we can rewrite Eq. (11) in the form

$$\frac{d(n-n_L)}{dt} = -\left(\frac{n}{\tau} - \frac{n_L}{\tau_L}\right). \quad (18)$$

Since we are allowing  $I$  to vary by only a few percent between the time when the square-wave pulse is on and the steady irradiance, we may assume that  $n$  will vary from  $n_L$  by only a few percent, and hence that  $\tau$  will vary from  $\tau_L$  by only a few percent. Hence it is allowable to expand  $\tau$  about  $\tau_L$  as a power series in  $n-n_L$ . We have

$$\tau = \tau_L + (d\tau/dn)_L(n-n_L) + \dots \quad (19)$$

We substitute this expression in Eq. (18) and find

$$\frac{d(n-n_L)}{dt} = -\frac{(n-n_L)}{\tau_L} \left[ 1 - \left( \frac{d \ln \tau}{d \ln n} \right)_L \right]. \quad (20)$$

From Eq. (20) we see that  $n-n_L$  will decay logarithmically, and that the time constant observed in the modulation experiment, which we shall call  $\tau_{\text{mod}}$ , is

$$\tau_{\text{mod}} = \tau_L \left[ 1 - \left( \frac{d \ln \tau}{d \ln n} \right)_L \right]^{-1}, \quad (21)$$

where  $\tau_L$  is the fundamental time constant of Eq. (11), in the presence of light. The derivative of  $\ln\tau$  with respect to  $\ln n$  is to be computed at the irradiance being used. In order to calculate the factor in Eq. (21), we shall assume that the time constant varies inversely as the conductivity, as in Eq. (12), and we shall assume that the conductivity is given in terms of  $n$  by the linear term of Eq. (9), disregarding the quadratic term, which is ordinarily small in the cases met in practice. Then we find that

$$(d \ln \tau)/(d \ln n) = -\ln(\sigma_L/\sigma_D), \quad (22)$$

so that Eq. (21) becomes

$$\tau_L = \tau_{\text{mod}}[1 + \ln(\sigma_L/\sigma_D)]. \quad (23)$$

From Eq. (23) we see that  $\tau_L$ , the time constant appearing in Eq. (11), is greater than that measured in the modulation experiment, by a factor which goes from unity at small irradiance, to something of the order of 6 or 7 at the highest irradiances used. This correction factor was not used in the experimental graphs shown in Fig. 10, but it was used in the values of  $\sigma_L\tau_L$  plotted in Fig. 13.

In the discussion of this modulation method of measuring time constant, it was assumed that the amplitude of the square-wave modulation was small enough so as to change the resistance of the sample by only a few percent. In the case of the high-resistance films, however, it was not possible to get measurements with such small modulations, and in some cases the change of conductivity produced by the modulation was very much larger than this value. This produced errors in the resulting values of time constant, which we have mentioned earlier, and which made the measurement of time constants of high-resistance films of very doubtful validity.

The second method of measuring time constant is a direct measurement of the decay of conductivity, as has been mentioned earlier. By a large steady irradiance, the conductivity is built up to perhaps several hundred times the dark conductivity. The irradiance is then removed, and the decay of the conductivity is observed. This should follow Eq. (11), in which  $I$  is set equal to zero. This allows us to find the time constant directly, if we assume as before that the conductivity and  $n$  are related by the linear term of Eq. (9). We then find

$$\frac{d \ln n}{dt} = \frac{1}{\tau} = \frac{d \ln \ln(\sigma/\sigma_D)}{dt}. \quad (24)$$

In other words, we need only plot  $\ln \ln(\sigma/\sigma_D)$  as a function of time, find the slope of this curve, and determine the time constant directly from it. This type of measurement has been carried out for only a few films, and while the results of it are in general agreement with the modulation method, it has not been used for detailed determination of time constants.

## 5. NUMERICAL AGREEMENT OF THEORY AND EXPERIMENT

In the preceding sections, we have seen that we have a general agreement between the barrier theory and experiment, though there are detailed points of disagreement. We have not, however, considered the values of the numerical constants involved, to see if they agree with expectations. In the present section we shall carry out such an investigation and shall find that the theory seems numerically reasonable. There are two constants whose reasonableness we shall consider:  $a$  of Eq. (11) and  $A$  of Eq. (12). We consider  $A$  first. To compute it, let us make the argument leading to Eqs. (11) and (12) more precise. Consider a trapped hole in a  $p$ -type region. There will be electrons surmounting the barrier, which can combine with it. The probability that an electron combine with it can be written as the recombination cross section, times the drift velocity of an electron, times the number of electrons per unit volume at the top of the barrier. This probability of recombination is what we have written as  $\sigma/A$ . On the other hand, the conductivity equals the number of electrons per unit volume at the top of the barrier, times  $e\mu$ . The drift velocity is  $(kT/2\pi m^*)^{1/2}$ . Hence we have

$$e\mu/A = c(kT/2\pi m^*)^{1/2}, \quad (25)$$

where  $c$  is the recombination cross section.

In Fig. 13 we plotted values of  $\sigma_L\tau_L$ , or of  $A$ , as a function of temperature, for a typical film. We can then use Eq. (25), together with the assumed mobilities of Table I, to compute the recombination cross section as a function of temperature, for this particular case. The results are shown in Table II. We see that these values vary somewhat with temperature, being smaller at high temperatures. No explanation is offered for this, but many fairly complicated mechanisms could be postulated which would lead to such results. The essential result, however, is the order of magnitude of the cross sections. Recombination cross sections have been observed all the way from a maximum of about  $10^{-13}$  cm<sup>2</sup> to much smaller values, as is pointed out by Rose.<sup>2</sup> Thus the values which we deduce from our model fall well within the expected range. Similar

TABLE II. Recombination cross section of trapped hole as function of temperature, film R19X.

$10^3/T$	Recombination cross section (cm <sup>2</sup> )
4	$3.8 \times 10^{-16}$
5	$1.7 \times 10^{-15}$
6	$6.5 \times 10^{-15}$
7	$2.1 \times 10^{-14}$
8	$3.8 \times 10^{-14}$
9	$4.5 \times 10^{-14}$
10	$4.8 \times 10^{-14}$
11	$4.2 \times 10^{-14}$

calculations on other films lead to cross sections in the same general range of values.

Next let us consider the constant  $a$ . This occurs in the statement that the number of electron-hole pairs created per second is  $aI$ , where  $I$  is the irradiance. Let us assume that a fraction  $\alpha$  of all photons falling on the sample produce electron-hole pairs. If we take the average wavelength of the photons to be  $2\ \mu$  (which is approximately the location of the maximum energy density in the spectrum of the light source), then the energy of a photon is about  $1.0 \times 10^{-19}$  joule. An irradiance of  $1\ \text{w/cm}^2$  will then correspond to about  $10^{19}$  photons per sec per  $\text{cm}^2$ . The average thickness of the films is about  $0.2\ \mu$ . If we assume that a fraction  $\alpha$  of the photons falling on a square centimeter per second is absorbed in this film, we shall find that the number of photons absorbed per second per cubic centimeter is  $5 \times 10^{23} \alpha$ , for an irradiance of  $1\ \text{w/cm}^2$ . This then gives us an estimate of  $a$ .

To compare with experiment, it was found that the constant value of  $(aD/N_0X)$ , used in computing Fig. 14 from Eq. (14), was  $5.3 \times 10^4\ \text{cm}^2/\text{w-sec}$ . We are assuming that  $D=0.1\ \mu$ . For the product  $N_0X$ , we can use Eq. (5),

in which  $E_0$  can be neglected in this case, giving a relation between  $N_0$ ,  $X$ , and the barrier height  $\Delta E_0$ , which was  $0.285\ \text{ev}$  in the case considered. These relations lead to

$$N_0X = 2(k\epsilon_0 N_0 \Delta E_0 / e^2)^{1/2}. \quad (26)$$

If we assume  $N_0=10^{18}/\text{cc}$ , we then find that  $a=1.76 \times 10^{22}$ , from which  $\alpha=0.035$ ; if we assume that  $N_0=10^{19}/\text{cc}$ ,  $\alpha=0.11$ . In other words, for reasonable choices of the impurity concentration, we find values of  $\alpha$ , the fraction of impinging photons which produce electron-hole pairs, of a few percent, which certainly seems plausible, when we consider that part of the incident radiation will be of too long wavelength to be absorbed, and much of the rest of it will be reflected or scattered, or will pass through the film (since it is not thick enough to be perfectly opaque). Our estimate of  $a$ , then, as of  $A$ , seems to lie in an entirely reasonable range of values, completing our discussion of the agreement of the barrier theory with experiment, and showing that it is able to give a reasonable account of the main features of the observed photoconductivity.